ELSEVIER

Polymer 43 (2002) 7497–7504

polymer

www.elsevier.com/locate/polymer

Entropy and fragility in vitreous polymers

A. Saiter[a], M. Hess[b], N.A. D'Souza[c], J.M. Saiter[a,*]

[a]*Laboratoire d'Etude et de Caractérisation des Amorphes et des Polymères, Faculté des Sciences, EA 1292, Université de Rouen, 76821 Mont Saint Aignan Cedex, France*

[b]*Department of Physical Chemistry, Gerhard Mercator University, D-47048 Duisburg, Germany*

[c]*Department of Materials Science, University of North Texas, Denton, TX 76203-5308, USA*

Abstract

The study of the sub T_g relaxation in a semi-rigid polymer family for which the size of the lateral chain varies from one carbon to three carbon atoms have been performed. We used an entropic model proposed by Hutchinson et al. [Macromolecules 33 (2000) 5252] introducing a new parameter x_s called the entropic non-linearity parameter. For our samples we found $x_s = 0.45 \pm 0.05$. On comparison with the data obtained on other linear polymers, we have shown that the rigidity of the main chain involves an increase in the entropic non-linearity parameter x_s. Furthermore, we have shown, by using the fragility concept, that this new entropic model is conceptually equivalent to the Random Walk Model proposed by Arkhipov et al. [J. Non-Cryst. Solids 172 (1994) 396; J. Phys. Chem. 98 (1994) 662].

Keywords: Entropy; Fragility; Ageing

1. Introduction

Cooling a liquid with a rate high enough to avoid crystallisation leads into the supercooled regime where the viscosity increases drastically as the temperature decreases. At a given temperature, or more precisely in a certain temperature range, almost all supercooled liquids can undergo a transition into a 'frozen-in' thermodynamical non-equilibrium state called a glass. This transition (kinetically controlled) is termed glass transition and the corresponding temperature is the glass transition temperature. The glass is characterised by an excess of free volume, an excess of enthalpy, and an excess of entropy, when comparison is made with the thermodynamic equilibrium state. As a direct consequence, a glass kept at $T < T_g$ looses its excess of entropy by molecular relaxation to reach the thermodynamic equilibrium state. This process is generally called structural relaxation or physical ageing [1] and may be illustrated using the entropic diagram displayed in Fig. 1a. In the same way, physical ageing interpreted in terms of enthalpy loss leads to the diagram presented as Fig. 1b. After an infinite ageing duration performed on a glass maintained at a temperature $T_a < T_g$, but closed to T_g, the expected enthalpy loss ΔH_∞ can be estimated by means of the following relationship

$$\Delta H_\infty = (C_{p_l} - C_{p_g})(T_g - T_a) \quad (1)$$

where C_{p_l} and C_{p_g} are the specific heat capacity of the equilibrium liquid and of the glass, respectively. Nevertheless, some experimental results show that the variations of enthalpy found after infinite ageing are lower than expected [2,3].

From an alternative method, using the Gibbs entropic model, Gomez Ribelles et al. [3,4] have found that the experimental curves obtained on samples of different thermal histories including physical ageing can be correctly fitted if a new term is introduced. This new term indicates that the amount of entropy loss observed after an infinite ageing is also lower than expected (Fig. 1c).

More recently, Hutchinson et al. [5] have introduced temperature dependencies for the entropy in the glassy state from the Adam–Gibbs equation relative to the non-equilibrium glassy state. The model assumes that only a certain fraction of either flexed bonds and/or vacant lattice sites (holes) are frozen-in at the glass transition. This temperature dependence for the entropy, shown by Fig. 1d, leads to an entropic non-linearity parameter x_s defined by:

$$S_c(T, T_f) = x_s S_c(T) + (1 - x_s) S_c(T_f) \quad (2)$$

Thus, the entropy $S_c(T, T_f)$ can be broken down into two different contributions, one represents the temperature

* Corresponding author. Tel.: +33-235-146632; fax: +33-235-146882.
E-mail address: jean-marc.saiter@univ-rouen.fr (J.M. Saiter).

0032-3861/02/$ - see front matter
PII: S0032-3861(02)00631-6

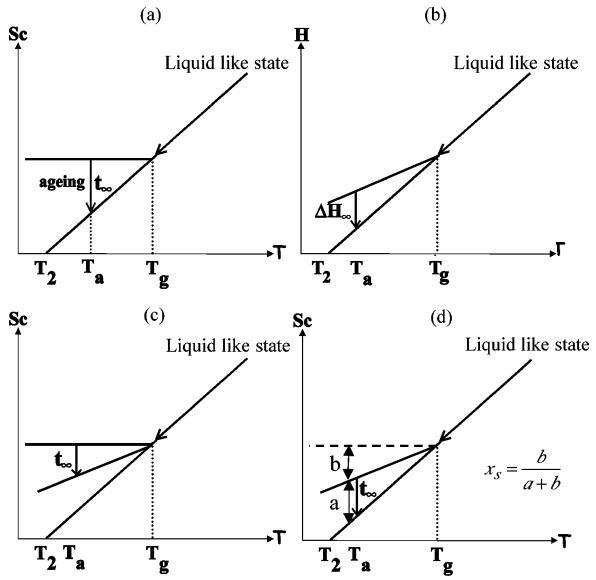

Fig. 1. T_a: the ageing temperature; T_g : the glass transition temperature; T_2 : the Kauzmann temperature. (a) Variations of the entropy after an infinite ageing time t_∞; (b) theoretical variations of the enthalpy after t_∞; (c) schematic variations of the entropy after t_∞ according to the model of Gomez Ribelles et al.; (d) schematic variations of the entropy after t_∞ according to the model of Hutchinson et al., and the definition of the parameter x_s.

contribution $S_c(T)$, and the second represents the structure contribution $S_c(T_f)$. As shown in Fig. 1d, the entropic non-linearity parameter x_s is defined by:

$$x_s = \frac{b}{a+b} \tag{3}$$

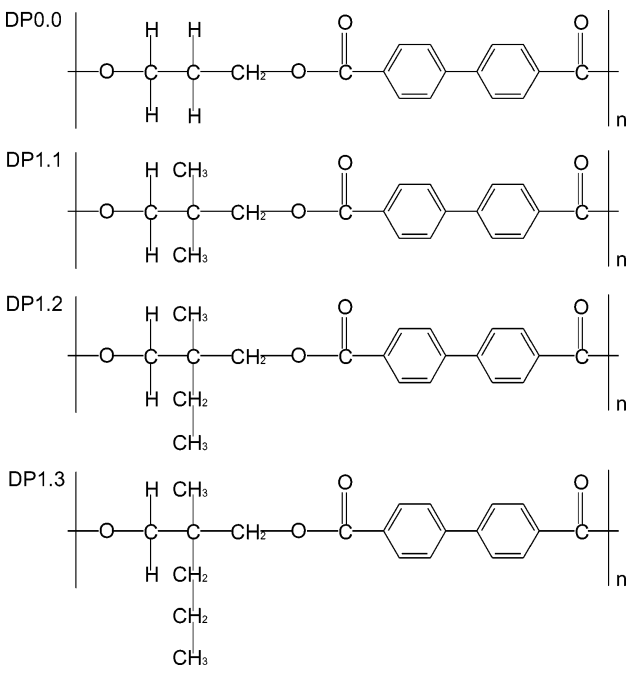

Fig. 2. Chemical formula of DP0.0, DP1.1, DP1.2 and DP1.3 samples.

If x_s is equal to 0, this model supposes that the liquid at T_g is completely frozen-in. If x_s is different from 0, this supposes that the liquid is only partially frozen-in. Furthermore, the parameter x_s is found to be linked to the non-linearity parameter x ($0 \leq x \leq 1$) defining the relative contributions of temperature and structure to the relaxation time given by the so-called Tool–Narayanaswamy–Moynihan equation (TNM) [6–8]

$$\tau = \tau_0 \exp\left(\frac{x\Delta h^*}{RT}\right)\exp\left(\frac{(1-x)\Delta h^*}{RT_f}\right) \tag{4}$$

where T_f is a fictive temperature characterising the structure of the glass and Δh^* is the apparent activation energy. The relationship linking x_s to x is

$$1 - x_s \cong (1-x)[1 + \ln(T_f/T_2)] \tag{5}$$

where T_2 is the Gibbs–DiMarzio temperature [9], equivalent to the Kauzmann temperature T_k. For instance, the value of this temperature can be obtained by fitting the variations of the viscosity versus temperature in the liquid state with the Vogel–Tamman–Fulcher (VTF) equation [10–12]

$$\eta = \eta_0 \exp\left(\frac{B}{T - T_2}\right) \tag{6}$$

where B is the activation energy, η_0 is the viscosity at infinite temperature.

In the following, using this approach we propose to analyse the results obtained from a family of liquid crystalline polymers with different lengths of the side chain. These polymers may be considered as semi-rigid polymers. From an experimental point of view, the different parameters that we have to determine can be obtained by calorimetric investigations. These materials exhibit the advantages that are [13] (i) a relative broad glass transition in temperature domain; (ii) a large endothermic peak characterising the enthalpy loss obtained after ageing; (iii) a high enough value for the ΔC_p jump at T_g. All these advantages drastically decrease the measurements uncertainties.

2. Experimental

2.1. Materials

The linear polymers studied in this work were synthesised in the Department of Physical Chemistry, Gerhard Mercator University, Duisburg. More information concerning the synthesis and the characterisation are given in Refs. [14–17]. The chemical formula is given in Fig. 2. The first sample is a poly[oxy(propane-1,3-diyl)carboxylbisphenyl-4,4′dicarbonyl] abbreviated DP0.0, and the other samples are poly[oxy(2,2dialkylpropane-1,3-diyl)carboxylbisphenyl-4,4′dicarbonyl] abbreviated DP1.1, DP1.2 and DP1.3, where the numbers indicate the number of carbons of the side chain attached to the tertiary carbon of the propyl

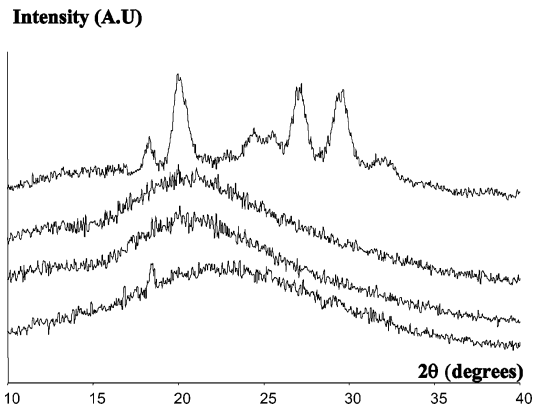

Fig. 3. Spectra obtained by X-ray diffraction. From buttom to top: DP1.3, DP1.2, DP1.1 and DP0.0.

spacer. A simple study by X-ray diffraction allows to affirm that the DP1.1, DP1.2 and DP1.3 samples show a clearly amorphous character, while the DP0.0 sample is highly crystalline. For these reasons, only DP1.1, DP1.2 and DP1.3 will be studied in this work. The different spectra are given in Fig. 3.

2.2. Thermal analysis

Differential scanning calorimetry (DSC) was performed with a Perkin–Elmer Series 7 calorimeter. Experiments were carried out under a nitrogen flow at a heating rate of 20 K/min. The calorimeter was calibrated with regard to temperature and energy with Indium and Zinc. Finally, to limit the statistical data scattering, all thermal cycles were made in situ with the same sample. We may notice that the value of $\Delta C_p(T_g)$ obtained for the first thermal cycle is the same than for the last one. As this quantity is very sensitive to the degree of crystallinity, this proves that no crystallisation occurs during our experimental procedure for all the studied samples.

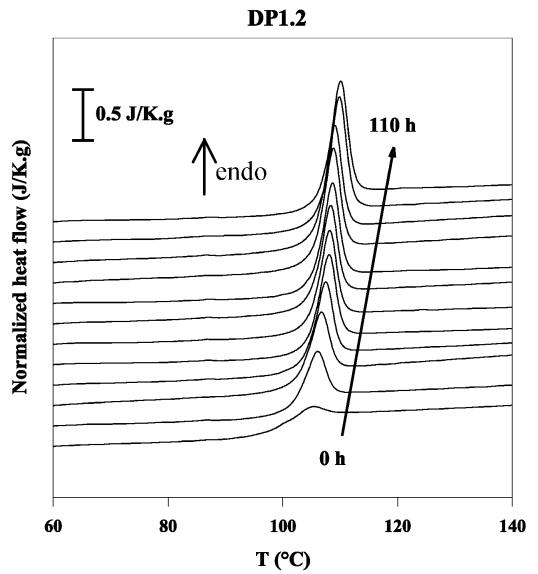

Fig. 4. DP1.2: DSC curves obtained after various annealing times. The ageing temperature is $T_a = T_g - 15$ K, the heating rate is $q^+ = 20$ K/min.

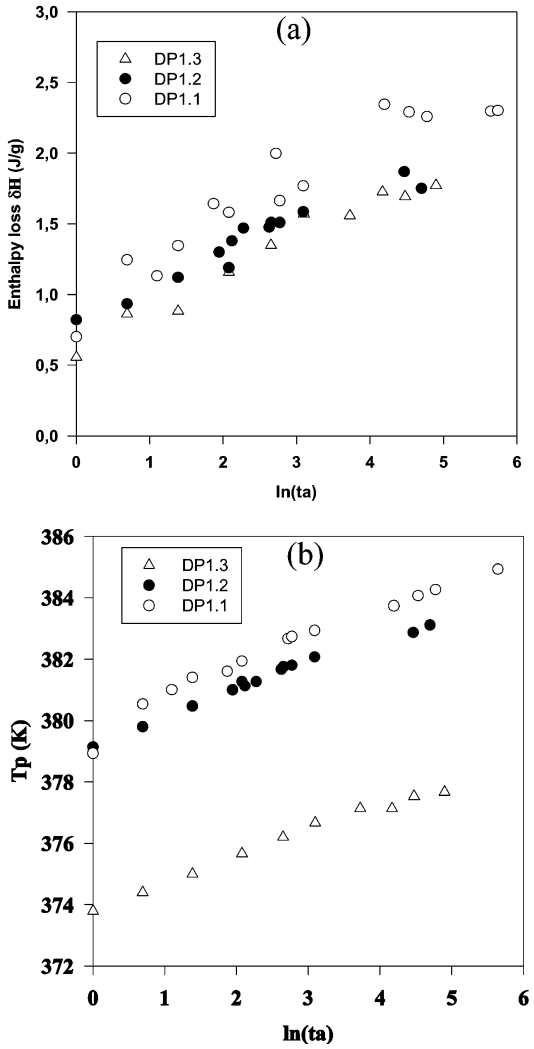

Fig. 5. (a) Variations of the enthalpy loss δH versus the ageing time for the three samples; (b) variations of the temperature T_p versus the ageing time for the three samples.

All parameters defined in relationship (4) can be determined from DSC experiments using the peak-shift method [18,19] to evaluate the non-linearity parameter x, and using the Moynihan method [8] to determine the fictive temperature T_f and the apparent activation energy Δh^*.

The peak-shift method has been applied successfully to other polymers [20–22] and inorganic glasses [23,24]. This method is based on the displacement toward higher temperatures of the endothermic peak associated with the structural relaxation at the glass transition, when samples are subjected to various ageing times (t_a) at a constant ageing temperature (T_a). All details of this method are specified in Refs. [18,19]. After the study of the dependence of the fictive temperature T_f on the cooling rate q^- in intrinsic cycles, the apparent activation energy Δh^* is

Table 1
Structural relaxation and VTF fit parameters for the DP1.*i* samples

	DP1.1	DP1.2	DP1.3
T_g (K); $q^+ = q^- = 20$ K/min	373.9	372.2	367.8
Δh^* (kJ/mol)	745 ± 79	771 ± 79	898 ± 38
Fragility index, m	104 ± 11	108 ± 11	122 ± 5
x	0.55 ± 0.05	0.53 ± 0.05	0.54 ± 0.05
Glass fragility index, m_g	57 ± 11	57 ± 11	66 ± 5
x_s	0.45 ± 0.05	0.43 ± 0.05	0.48 ± 0.05
T_2 (K)	301.8	299	321.6
B (K)	1572	1610	1035
η_0 (Pa s)	0.17	4.1×10^{-3}	0.41
$T_g - T_2$ (K)	72.1	73.2	46.2

obtained according to the following equation [8]:

$$\frac{d(\ln|q^-|)}{d(1/T_f)} = \frac{-\Delta h^*}{R} \quad (7)$$

2.3. Viscosity measurements

Complex viscosity was measured on a Paar Physica UDS200 between 0.1 and 100 rad/s at temperatures ranging from 423 to 473 K. A parallel plate configuration and an angular strain of 1% were determined to be well within the linear viscoelastic region in preliminary testing. Measurements were performed at the University of North Texas (Denton, Department of Materials Science).

3. Results

Fig. 4 shows the glass transition observed by DSC and obtained for the DP1.2 sample as an example, annealed at $T_g - 15$ K for ageing times t_a as indicated. These experimental data allow the determination of the non-linearity parameter x. First, we can say that the DP1.2 sample shows a classical behaviour: the longer the ageing time, the more intensive the endothermic relaxation peak (involving a higher enthalpy loss), and the higher the temperature T_p. This temperature corresponds to the maximum of the relaxation endothermic peak at the glass transition. For the samples DP1.1 and DP1.3, we have observed exactly the same phenomena. We specify that the ageing duration varies from 1 to 283 h for sample DP1.1 and from 1 to 134 h for sample DP1.3. According to the peak shift method, the variations of the enthalpy loss (δH) and the endothermic peak temperature T_p with the ageing time t_a (Fig. 5) lead to the values of the non-linearity parameter x reported in Table 1. For the three samples, practically the same value $x = 0.55 \pm 0.05$ is found.

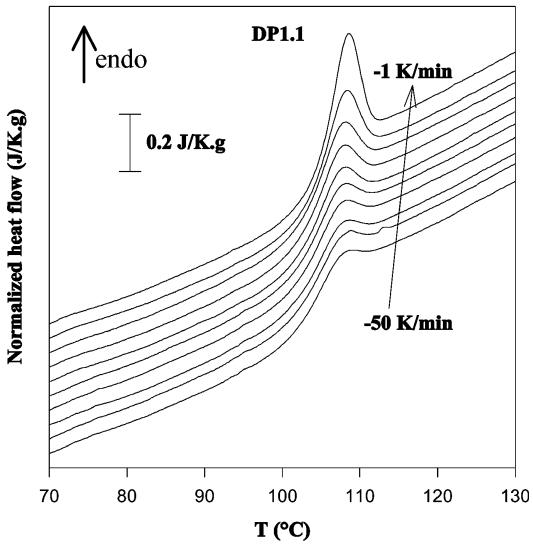

Fig. 6. DP1.1: DSC curves obtained with a heating rate $q^+ = 20$ K/min after various cooling rate.

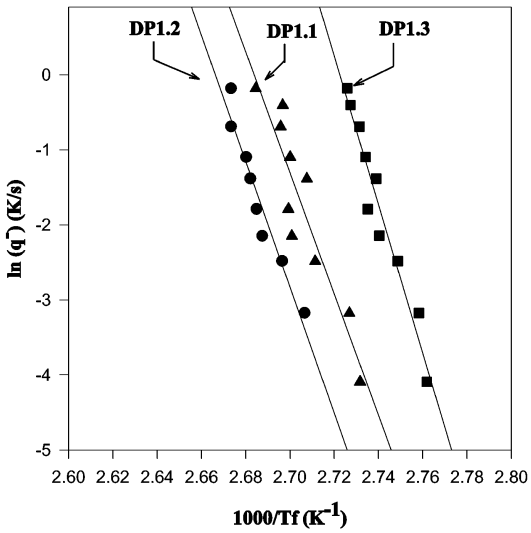

Fig. 7. Determination of Δh^* : variations of $\ln q^-$ with $1000/T_f$ for DP1.*i* samples.

Fig. 6 shows the DSC curves obtained at a constant heating rate $q^+ = 20$ K/min for sample DP1.1, successively cooled at the indicated cooling rate q^-. These experimental data can be used to determine the apparent activation energy Δh^*. We observed that the endothermic peak, produced at the glass transition and characteristic of the relaxation phenomenon, increases with decreasing cooling rate. For the DP1.2 and DP1.3 samples, we have made the same observations [13]. The fictive temperature T_f was evaluated for each curve according to the Moynihan method [8] and the dependence of reciprocal T_f on $\ln|q^-|$ is shown in Fig. 7 for the three samples. In Table 1, we have reported the values of the apparent activation energy and the values of the glass transition temperature T_g determined for $q^+ = q^- = 20$ K/min. For samples DP1.1, DP1.2 and DP1.3, we find, respectively, $T_g = 373.9$ K and $\Delta h^* = 745 \pm 79$ kJ/mol, $T_g = 372.2$ K and $\Delta h^* = 771 \pm 79$ kJ/mol, $T_g = 367.8$ K and $\Delta h^* = 898 \pm 38$ kJ/mol. We observe that when the length of the lateral chain

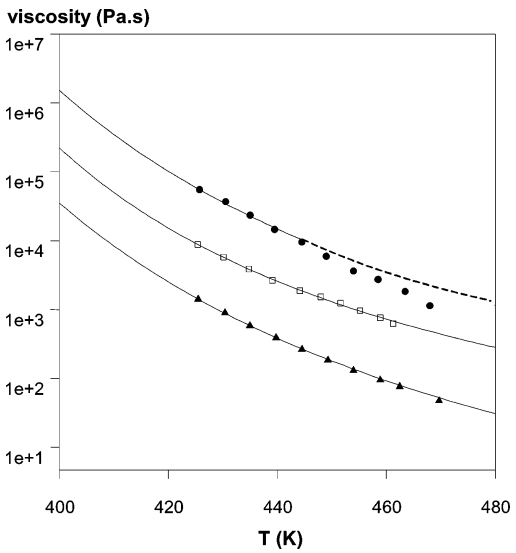

Fig. 8. Variations of the viscosity versus temperature for the three samples: (●) DP1.1; (□) DP1.2; (▲) DP1.3. The full lines represent the VTF type fits and the dashed line represents the smectic behaviour range for the DP1.1 sample.

increases, the apparent activation energy increases whereas the glass transition temperature decreases.

In order to determine the entropic non-linearity parameter x_s, we have to know the value of the Gibbs–DiMarzio temperature T_2. Fig. 8 shows the variation of the viscosity on a logarithmic scale versus temperature for the three samples. The plots correspond to the experimental measurements and the full lines correspond to the VTF law fitting for each series of experimental data. For DP1.2 and DP1.3 samples, we obtain a very good fit but for the DP1.1 sample a breaking appears at approximately 440 K (dashed line in Fig. 8). This phenomenon can be explained by a smectic transition, which begins around this temperature

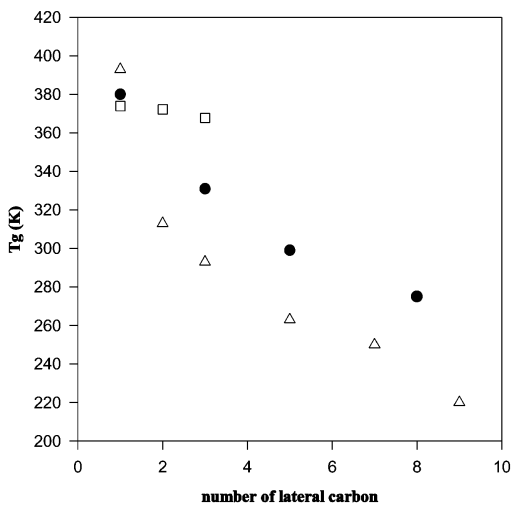

Fig. 9. Variations of the glass transition temperature versus the number of carbon atoms in the lateral chain for three family samples: our samples called DP1.*i* (□) the poly(α-*n*-alkyl)acrylates called C*i* (●) [27] and the polymethacrylates *n*-alkyl (△) called C′*i* [28].

[25]. To determine the VTF law parameters in this case, we have only used the experimental points determined at temperatures lower than 440 K. All VTF fit parameters are reported in Table 1. For this work, the most important VTF parameter is the Gibbs–DiMarzio temperature T_2, and a means to judge the quality of the evaluated values is to calculate the difference $(T_g - T_2)$. In our case, we find 72.1 K for DP1.1, 73.2 K for DP1.2 and 46.2 K for DP1.3. These differences are reasonable considering the reported results for viscoelastic or dielectric relaxation times in the main relaxation process [26]. Having the values of the fictive temperature T_f, the non-linearity parameter x and the Gibbs–DiMarzio temperature T_2, we can estimate the value of the x_s parameter from Eq. (5). According to the standard deviation of the x_s values, we can conclude that there is no change for the DP1.*i* samples when the carbon number varies from 1 to 3 in the lateral chain: $x_s \cong 0.45 \pm 0.05$ for the three samples.

4. Discussion

The first parameter discussed is the glass transition temperature T_g. We have found for DP1.*i* samples that the value of the glass transition temperature decreases slowly when the length of the lateral chain increases. Fig. 9 shows the decrease in the glass transition temperature with increasing length of the side chain for two other linear polymeric systems [27,28]. Indeed, if the rigidity of the lateral chain is important, they behave as spacers. Thus, an increase in their size involves a strong decrease of the interchain interactions so that the glass transition temperature decreases.

Concerning the value of the non-linearity parameter x, we have found no dependence on the length of the lateral chain for our three samples. According to Eq. (4), the value of $x = 0.55 \pm 0.05$ means that basically the temperature effects and the structural effects influence the relaxation process practically in the same way. Since different experimental conditions can lead to different x values for the same material, we have voluntarily limited the comparison of our data to others obtained on poly(α-*n*-alkyl)acrylates in the same experimental conditions [20]. The data are reported in Table 2. x varies from 0.3 to 0.6 as expected for the major part of linear polymers [29]. For the poly(α-*n*-alkyl)acrylates, the value of x changes when the number of carbon atoms on the lateral chain is greater than three. This threshold separating two distinct types of behaviour was observed for this linear polymer class with respect to many properties [2,20,30]. For less than five methylene groups in the lateral chain, the value of the non-linearity parameter x is equal to 0.30 ± 0.04. This value is smaller compared with the value found for the DP1.*i* samples at equivalent lateral chain length ($x = 0.55 \pm 0.05$). In terms of molecular interactions, it was shown that, when experiments are performed in the same way on a large

Table 2
Structural relaxation parameters for the poly(α-*n*-alkyl)acrylates

	C1	C3	C5	C8
T_g (K)	380	331	299	275
Δh^* (kJ/mol)	873 ± 75	856 ± 75	524 ± 66	391 ± 75
Fragility index, m	120 ± 11	135 ± 13	92 ± 13	75 ± 15
x	0.37 ± 0.04	0.35 ± 0.03	0.52 ± 0.06	0.58 ± 0.06
Glass fragility index, m_g	44 ± 11	47 ± 13	48 ± 13	43 ± 15
T_2 (K)	325	291	255	222
$T_g - T_2$ (K)	55	40	44	53
x_s	0.29 ± 0.04	0.28 ± 0.03	0.45 ± 0.06	0.51 ± 0.06

diversity of materials for which structural parameters are well identified, greater intermolecular forces result in lower x values [29,31]. This means that the molecular interactions are more important for the relaxation process of poly(α-*n*-alkyl)acrylates compared with the corresponding DP1.*i* samples. This conclusion is coherent in regard to the chemical structure of the molecules engaged into the macromolecular edifice. These results also show that the sensitivity of the non-linearity parameter x to change with structural modifications is relatively small. Thus, no strong correlation between x and structural parameters is evident.

Fig. 5 shows that the enthalpy loss decreases with increasing lateral chain length from one carbon to three carbon atoms after equivalent annealing. As the value of the differential heat capacity at the glass transition is the same for all three DP1.*i* samples ($\Delta C_p(T_g) = 0.21 \pm 0.02$ J/K g [13]), this means that our three samples exhibit the same thermodynamic imbalance but under the same ageing conditions, the structural relaxation kinetics are faster for DP1.1 sample than for DP1.2 and DP1.3 samples.

As previously mentioned, the calculation of the entropic non-linearity parameter x_s requires the knowledge of the Gibbs–DiMarzio temperature T_2. From the data reported in Table 1 and according to relationship (5), we have determined x_s for our samples and we have found a constant value for the three samples $x_s = 0.45 \pm 0.05$. In the same way, we have determined x_s for the poly(α-*n*-alkyl)acrylates and the values are reported in Table 2. The evolution of the entropic non-linearity parameter x_s versus the length of the lateral chain is shown in Fig. 10. For the poly(α-*n*-alkyl)acrylates we observe an increase in the x_s parameter as the length of the lateral chain increases: x_s values vary from 0.29 ± 0.04 to 0.51 ± 0.06. The entropy excess at the glass transition decreases with increasing lateral chain length. According to this model, an increasing of the value of x_s implies that the intermolecular interactions increase when the length of the lateral chain increases, and that the contribution of vacant lattice sites (holes) is more important than the contribution of flexed bonds during the structural relaxation process. Now, if we compare the two polymer types at equivalent lateral chain length (from one carbon to three carbons), the rigidity of the main chain involves an increasing entropic non-linearity parameter x_s, (0.3 → 0.45), and consequently, a decreasing excess entropy when the glass is formed. Furthermore, we can observe that the effects of the main chain rigidity on x_s can be compensated by the effects of the lateral chain length. Indeed, for the poly(α-*n*-alkyl)acrylates, we found $x_s = 0.45 \pm 0.05$ when the length is greater than three carbons, and this value corresponds to those obtained for the DP1.*i* samples.

In fact, this entropic model proposed by Hutchinson et al. [5] can be linked to the random walk model (RWM)

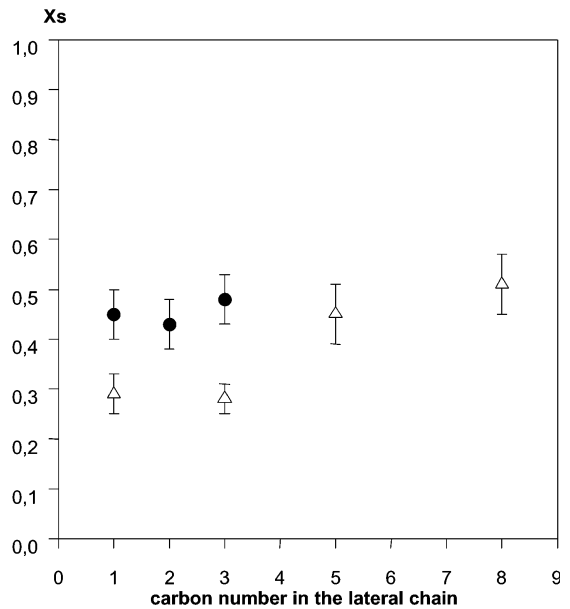

Fig. 10. Evolution of the parameter x_s versus the length of the lateral chain for our samples called DP1.*i* (●), and for the poly(α-*n*-alkyl)acrylates called C$_i$ (△).

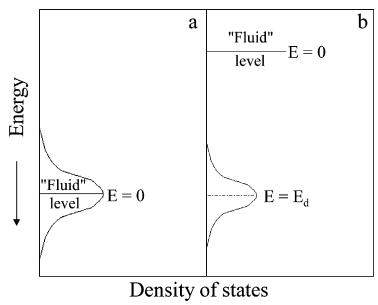

Fig. 11. Energetic distributions of metastable states for (a) weakly bonded (fragile) and (b) strongly bonded (strong) liquids.

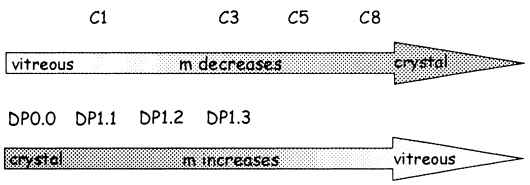

Fig. 12. Evolution of the fragility index m with the crystallisation ability for the poly(α-*n*-alkyl)acrylates (from C1 to C8) and for our samples (from DP0.0 to DP1.3).

proposed by Arkhipov et al. [32,33]. The RWM model assumes the existence of two types of excitations in viscous liquids: elastic excitations, which do not contribute to viscous flow, and inelastic excitations involving strong interactions between the molecules in viscous liquids. A transition from one configuration to another may be considered as a jump of a structural unit from one site to another in a highly complex energy landscape. Fig. 11a and b show the density of possible metastable states (DPMS) for two kinds of liquid. In weakly interacting liquids, there is no energy gap separating the 'fluid level' from metastable states (Fig. 11a). The fluid level states allow for transports of structural units in configurational space without further activation. For strongly interacting liquids the DPMS is lower and the fluid level is separated from metastable states by a broad energy gap (Fig. 11b). This energy gap E_d can be compared to the bond breaking energy. As already mentioned by Arkhipov et al., these two kinds of liquid correspond, respectively, to the fragile and strong glass forming liquids defined by Angell [34]. According to these models, we can say that the stronger the glass-forming liquid, the less liquid-like state is frozen-in at the glass transition. According to the definition proposed by Ngai et al. [35], a fragility index m for a glass forming liquid can

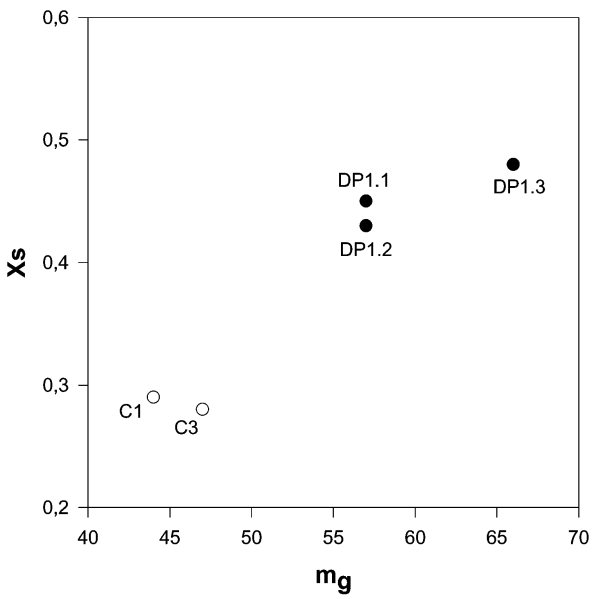

Fig. 13. Evolution of the data pairs (x_s–m_g) for our samples and for the poly(α-*n*-alkyl)acrylates at equivalent lateral chain length.

be obtained from

$$m = \left.\frac{\mathrm{d}\log_{10}(\tau)}{\mathrm{d}(Tg/T)}\right|_{T=T_g} \tag{8}$$

where τ is the relaxation time and T_g is the glass transition temperature obtained for q^+ (the heating rate) equal to q^-. By using Eqs. (4) and (8), it is easy to show that the fragility index m can be written as:

$$m = \frac{\Delta h^*}{RT_g \ln 10} \tag{9}$$

When the glass is formed, another fragility index called the glass fragility index can also be defined as [36]:

$$m_g = mx \tag{10}$$

Thus, if these models are similar, we have to verify that the small x_s values correspond to a stronger glass formation, and consequently, a smaller glass fragility index m_g. To this end, we have determined the fragility indexes m and m_g of our samples and compared with those obtained for the poly(α-*n*-alkyl)acrylates and the values are given in Tables 1 and 2. For the samples DP1.1, DP1.2 and DP1.3, we find, respectively, $m = 104 \pm 11$ and $m_g = 57 \pm 11$, $m = 108 \pm 11$ and $m_g = 57 \pm 11$, $m = 122 \pm 5$ and $m_g = 66 \pm 5$. Thus, when the length of the lateral chain increases in DP1.*i* samples, the glass forming liquid becomes more and more fragile. First, this result seems to be surprising by comparison with those obtained for the poly(α-*n*-alkyl)acrylates. Indeed, for this series of samples, the fragility index varies from $m = 120 \pm 11$ to 75 ± 15 when the length of the lateral chain varies from 1 to 8 carbon atoms. But, for the poly(α-*n*-alkyl)acrylates, when the length of the lateral chain approaches 12 carbons, the sample can crystallise easily. Accordingly, when the length of the lateral chain increases, the covalent type interactions become dominant and the sample becomes more and more strong (m decreases). For our samples, it was shown by X-ray diffraction that the sample noted DP0.0 has a significant crystallinity (Fig. 3). Consequently, when the length of the lateral chain increases, the covalent type interactions decrease and the samples become more and more fragile (m increases). Scheme 1 presented in Fig. 12 allows to compare the evolution of the fragility index between the two classes of glass forming liquids and allows to show that our results on the fragility index are consistent. Concerning the glass fragility index m_g, there is no evolution for the DP1.*i* samples if we consider the standard deviation on each value. We find $m_g \cong 60$. The same can be stated for the poly(α-*n*-alkyl)acrylates, for which $m_g \cong 45$. Thus, from the fragility point of view, different glass forming liquids can form like glasses. To verify that the RWM and the Hutchinson's model lead to similar conclusions, we have plotted in Fig. 13 the glass fragility indexes m_g versus the entropic non-linearity parameter x_s for the two polymer classes, at equivalent lateral chain length. We observe that at a small

value of m_g corresponds a small value of x_s; the stronger the glass, the higher the number of flexed bonds which is frozen-in at the glass transition involving a more disordered state in the glass. It appears that the model proposed by Hutchinson et al. [5] is coherent with the RWM proposed by Arkhipov et al. [32,33] in regard to the fragility concept [34].

5. Conclusion

In this work, for two families of linear polymers in which the same structural parameter is changed, we have determined the fragility of these samples and the new entropic non-linearity parameter x_s proposed by Hutchinson et al. by studying the sub T_g relaxation. By making a comparison between the glass fragility index m_g and the entropic non-linearity parameter x_s, we have shown that the entropic model proposed by Hutchinson et al. and the RWM proposed by Arkhipov et al. are in good agreement.

Acknowledgements

We thank Dr Mehrdad Negahban for carefully reading the manuscript.

References

[1] Struik LCE. Physical aging in amorphous polymers and others materials. Amsterdam: Elsevier; 1978.
[2] Godard ME, Saiter JM. J Polym Sci, Part B: Polym Phys 1998;36:2865.
[3] Gomez Ribelles JL, Monleon Pradas M. Macromolecules 1995;28:5867.
[4] Gomez Ribelles JL, Monleon Pradas M, Vidaurre Garayo A, Romero Colomar F, Mas Estelles J, Meseguer Duenas JM. Macromolecules 1995;28:5878.
[5] Hutchinson JM, Monserrat S, Calventus Y, Cortes P. Macromolecules 2000;33:5252.
[6] Tool AQ. J Am Ceram Soc 1946;29:240.
[7] Narayanaswamy OS. J Am Ceram Soc 1971;54:491.
[8] Moynihan CT, Easteal AJ, De Bolt MA, Tucker J. J Am Ceram Soc 1976;59:12.
[9] Gibbs JH, DiMarzio EA. J Chem Phys 1958;28:373.
[10] Vogel H. Physik Z 1921;22:645.
[11] Tamman G, Hesse G. Z Anorg Allg Chem 1926;156:245.
[12] Fulcher GS. J Am Chem Soc 1925;8339:789.
[13] Saiter A, Hess M, Saiter JM, Grenet J. Macromol Symp 2001;174:165.
[14] Woelke R, Hess M. Polym Engng Sci 1999;39:519.
[15] Baxmann R, Hess M, Woelke R, Veeman W. Macromol Symp 1999;148:157.
[16] Stickfort L, Poersch G, Hess M. J Polym Sci, Polym Chem 1996;34:1325.
[17] Hess M. Mater Res Innov 2002;6:31.
[18] Ramos AR, Hutchinson JM, Kovacs AJ. J Polym Sci, Polym Phys Ed 1984;22:1655.
[19] Hutchinson JM. Molecular dynamics and relaxation phenomena in glasses. Lecture notes in physics, vol. 277. Berlin: Springer; 1987. p. 172.
[20] Godard ME, Saiter JM, Cortes P, Monserrat S, Hutchinson JM, Burel F, Bunel C. J Polym Sci, Part B: Polym Phys 1998;36:583.
[21] Morancho JM, Salla JM. J Non-Cryst Solids 1998;235:596.
[22] Cortes P, Monserrat S, Hutchinson JM. J Appl Polym Sci 1997;63:17.
[23] Cortes P, Monserrat S, Ledru J, Saiter JM. J Non-cryst Solids 1998;235:522.
[24] Hutchinson JM, Ingram MD, Pappin AJ. J Non-Cryst Solids 1991;131:483.
[25] Woelke R, Hess M. Polym Engng Sci 1999;39:3.
[26] Ferry JD. Viscoelastic properties of polymers. New York: Wiley; 1970.
[27] Godard ME, Saiter JM. J Non-Cryst Solids 1998;235:635.
[28] Yoshida H, Kobayashi Y. J Macromol Sci Phys 1982;21:565.
[29] Saiter JM, Denis G, Grenet J. Macromol Symp 1999;148:15.
[30] Grenet J, Saiter JM, Godard ME. J Non-Cryst Solids 2002;232:307–10.
[31] Cortes P, Monserrat S. J Non-Cryst Solids 1994;172:622.
[32] Arkhipov VI, Bässler H. J Non-Cryst Solids 1994;172:396.
[33] Arkhipov VI, Bässler H. J Phys Chem 1994;98:662.
[34] Angell CA. J Phys Chem Solids 1988;49:863.
[35] Ngai KL, Rendell RW, Pye LD, Lacourse WC, Stevens HJ. The physics of non-crystalline solids. London: Taylor & Francis; 1992. p. 309.
[36] Hutchinson JM. Polym Int 1998;47:56.